eISSN 2330-0272



VEDIC RESEARCH INTERNATIONAL

Bioinformatics & Proteomics

JOURNAL HOME PAGE AT WWW.VEDICJOURNALS.COM

RESEARCH ARTICLE

DOI: http://dx.doi.org/10.14259/bp.v1i1.44

Pharmacophore Modelling, 3D-QSAR Study and Docking of Naphthol derivatives as B-Raf^(V600E) Receptor Antagonists

Khunza Meraj¹, Kukkala Kiran Kumar¹, Mohamed Sidig Shaikheldin¹, Soltani Nejad Azam¹, Parvathgari Reddy Anugnya¹, Manoj Kumar Mahto^{1,2,3*}, Matcha Bhaskar³

Article Info

Received: July 6th, 2013 Revised: July 13th, 2013 Accepted: July 16th, 2013

Keywords

Cancer

Pharmacophore modelling, 3D-QSAR, B-Raf^[V600E], Docking, Raf selective pocket,

ABSTRACT

B-Raf^(V600E) is a member of RAF kinase family involved in the ERK/MAP kinase pathway which regulates cellular proliferation, differentiation and survival. A single point mutation of Glutamic acid at position 600 can turn BRAF into an oncoprotein. 3D-QSAR (quantitative structure-activity relationship) and molecular docking approaches were performed on naphthol derivatives to understand their structural requisites and binding mode of the best fitted ligand for B-Raf^(V600E) inhibitory activity. Five featured pharmacophore *ADDRR.43* was considered to be the best hypothesis which yielded a statistically significant 3D-QSAR model built with 1A° grid spacing, PLS factor-2, Regression coefficient (R²) =0.9919, Cross validation coefficient (Q²) =0.6749, Root Mean Square Deviation (RMSD) =0.5382, Pearson-R=0.9081. The compound 11 is found to be the best fitted ligand for this hypothesis and was subjected to docking study which suggested that the hydrogen bonds, hydrophobic bonds and electrostatic interactions were closely related to B-Raf^(V600E) inhibitory activity and are in compliance with the predicted model. The geometry and features of this pharmacophore model emphasizes important binding features which will be useful for the design of selective B-Raf^(V600E) antagonists.

INTRODUCTION

BRAF is a human gene that codes for B-Raf protein. B-Raf is involved in sending signals from extracellular space through receptor tyrosine kinases (RTKs) to the nucleus in order to promote the expression of genes involved in cell growth, proliferation and survival. These proteins are found to be faulty

*Corresponding Author

Manoj Kumar Mahto (PhD)

Division of Animal Biotechnology, Department of Zoology, Sri Venkateshwara University, Tirupati, AP, India

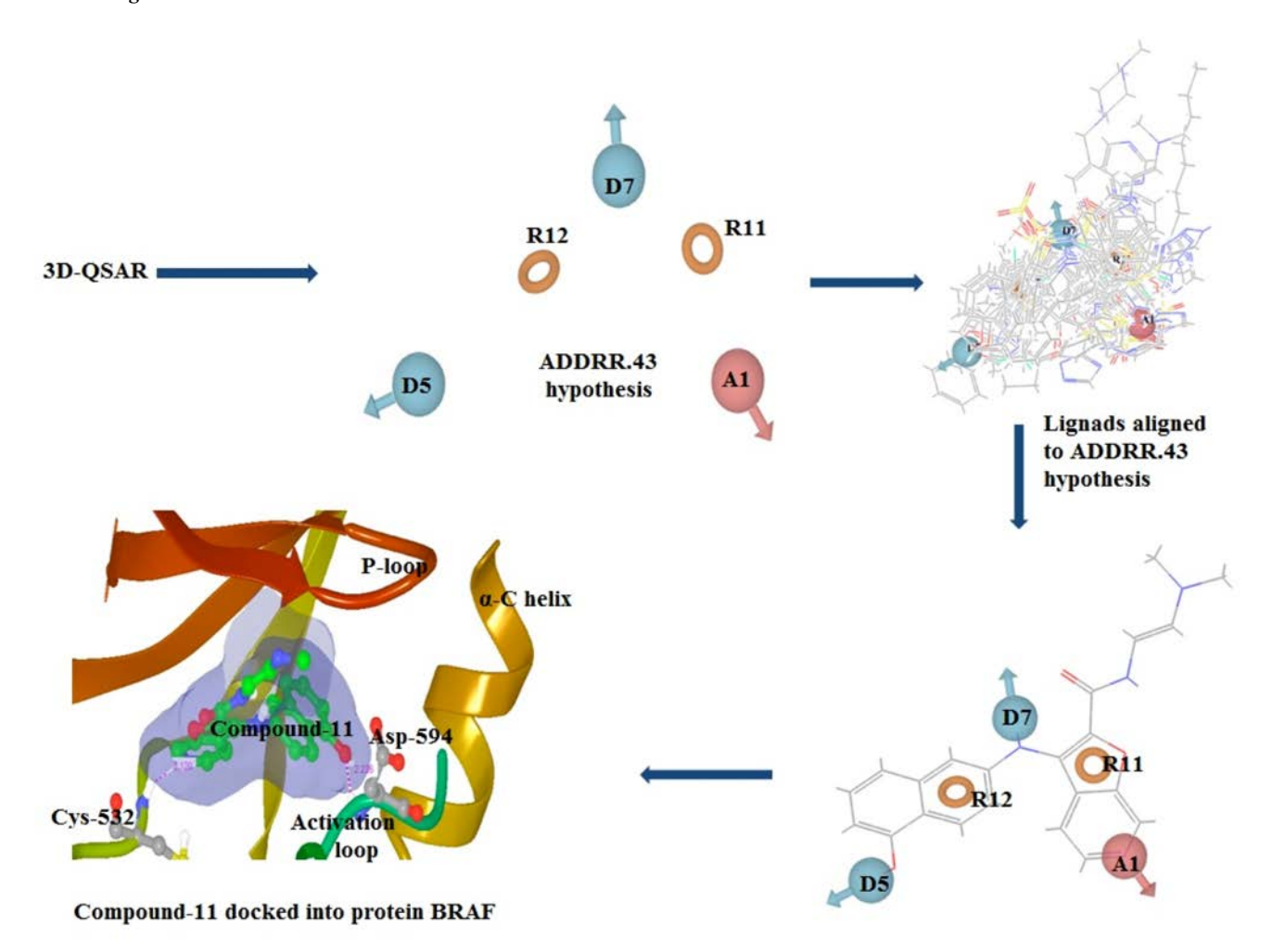
Phone: +91-9885928832 Email: <u>manoj4bi@gmail.com</u> (mutated) in about half of the malignant melanomas and other cancers and a kinase activating single valine to glutamate substitution at residue 600 (B-Raf^(V600E)) accounts for 90% of BRAF-mediated cancers. Mutations at the position V600 of BRAF were described in approximately 8% of all solid tumors, including 50% of melanomas, 30 to 70% of papillary thyroid carcinomas and 5 to 8% of colorectal adeno-carcinomas [1-2]. In Cancer cells, B-Raf^(V600E) is ~500-fold more active than wild-type protein and can stimulate constitutive ERK activity and drives proliferation and survival which leads to essential tumor growth and maintenance functions. Overall, these data suggest B-Raf^(V600E) as therapeutic target offering opportunities for anticancer drug development.

¹Aravinda Biosolutions, Hyderabad, AP, India

²Department of Biotechnology, Acharya Nagarjuna University, Guntur, AP, India

³Division of Animal Biotechnology, Department of Zoology, Sri Venkateswara University, Tirupati, AP, India

Abstract Figure



To reduce the overall cost associated with the new drug discovery and development, the computer-aided molecular designing methods have been identified as the most promising candidates to focus on the experimental efforts in modern medicinal chemistry. In the absence of structural data of the target receptor, pharmacophore mapping is one of the major elements of drug design. The idea is to provide useful pharmacophoric information for the future efforts in the development of more potent molecules in the series of Naphthol derivatives and to get insight into the structural and molecular properties. With this aim, the ligand-based 3D-QSAR study was performed using pharmacophore techniques with PHASE module from Schrödinger (Molecular Modeling Interface Inc., NY, USA) [3].

Development of potential inhibitors for a target protein is a complex multi-step process that involves screening of a large number of compounds for potential 'hits' in relevant assays. Information obtained from these hits is useful for medicinal chemists to design and synthesize compounds to identify novel molecules or optimize compounds into suitable leads that can be tested in preclinical experiments. Available chemical libraries are expanding rapidly due to combinatorial chemistry thus

allowing exploration for inhibitors in new chemical space. However, identification of hits from assay screens of vast libraries can be costly process. One way to reduce cost is to limit screening to a focused library of compounds that represent the chemical space of interest constituted by related chemotypes. Several thousand compounds can be rapidly synthesized with advances in combinatorial synthesis technology, thus expanding the relevant chemical space [4]. Hence, predictive models like QSAR (Quantitative Structure Activity Relationship) are helpful to prioritize compounds for screening, aid rational synthesis and facilitate lead identification [5].

The three-dimensional pharmacophore study can explain the activity of a series of ligands, which is one of the most significant contributions of computational chemistry to drug discovery [6]. A QSAR model is useful in relating biological activity to physico-chemical and structural descriptors of compounds. Application of QSAR techniques for identification of lead compounds have been widely used for a wide range of biological targets [7]. A 3D-QSAR model is built using the alignment of three dimensional conformers of active compounds and can be subsequently used to score a candidate compound on the basis of a fitting function that evaluates the

alignment of three dimensional chemical features to the model [8-10]. A pharmacophore is constituted of common chemical features (such as hydrogen donors, hydrogen acceptors, hydrophobic groups, charged groups and aromatic rings) that are distributed spatially to interact with the biological target and exert activity [11]. Development of 3D pharmacophore models based on the biological activity of compounds enables ligand-based drug design that guides experimental chemical synthesis of compounds with higher potency even when the 3D structure of the biological target is unknown [12].

Identification of pharmacophore is the most important step in rational drug design for achieving a stipulated goal. Pharmacophore alignment and scoring engine (PHASE) software was used to develop ligand based pharmacophore model for B-Raf^(V600E). PHASE uses conformational sampling and different scoring techniques to identify common pharmacophore hypothesis, where each hypothesis is accompanied by a set of aligned conformations which are necessary for ligand to bind to the receptor [13]. The conformations of active compounds that are obtained from alignment of pharmacophoric points are used to derive 3D-QSAR models. Further, docking study is performed using GLIDE 5.7 to check the binding modes of best fitted ligand in our 3D-QSAR study with the active site amino acid residue of B-Raf^(V600E).

MATERIALS AND METHODS

Data Set

A total of 24 previously synthesized and evaluated Napthol derivatives were considered for the study. The in vitro biological data of 19 Naphthol compounds as B-Raf^(V600E) receptor antagonists identified by Jie Qin et.al (2012) [14] that preferentially inhibit B-Raf^(V600E) over B-Raf^(WT) and 5 Naphthol inhibitors developed for B-Raf^(V600E) by Li Ren et.al (2011) [15] are subjected for this insilico analysis. The computational work was run on a 2.40 GHz Intel core i3 system. The ligand preparation, protein preparation, grid generation, ligand docking and 3D QSAR was run from Schrödinger 2011 software. The 24 Naphthol derivatives were designed in

Figure 1: Basic structures of the Naphthol inhibitors (a, b)

a. (E)-N-(4-Oxonaphthalen-1(4H)-ylidene)sulfonicamide

b. 6-(furo[2,3-C]Pyridin-3-ylamino)naphthalene-1-ol

ChemBioOffice 2010 software and saved in mol format. The basic structures of the Naphthol derivatives are shown in Figure 1 (a, b) and the various substituents are listed in supplementary material (Table 1a & 1b).

PHASE Methodology

The 3D-QSAR study was carried out using PHASE [16]. It is an ideal tool for structure alignment, pharmacophore perception, activity prediction, and 3D database searching. Phase provides support for structure-activity relationship development (SAR), lead optimization, lead expansion and lead discovery. It executes fine conformational sampling and a range of scoring techniques to identify common pharmacophore hypotheses. The common pharmacophore hypotheses display characteristics of 3D chemical structures that are meant to be critical for binding. It is also well suited to drug discovery projects for which no receptor structure is available. A given hypothesis along with known activity data will create 3D-QSAR models that identify overall aspects of molecular structure for potent activity. These models may be used in conjunction with our hypothesis, a 3D database for molecules that are most likely to exhibit strong activity toward the target [17].

Preparing Ligands

The molecules were processed with LigPrep2.5 program for structure optimization and energy minimization. A number of conformers per structure were generated by using force field OPLS-2005 and RMSD 1.0 A°. The conformer with least potential energy was subjected for the further study. Then low energy conformation of each ligand were selected and subjected to Impact minimisation by Impact 5.7 to minimise the energy of ligands further. The prepared structures were imported to PHASE along with their activity values to develop pharmacophore model. All the compounds used in study have known IC50 values of different range therefore the values (in moles/litre) were converted into negative logarithm of IC₅₀ (pIC₅₀). The pIC₅₀ ranged from 9.0 to 5.215, of which pIC₅₀ above 7.0 were considered as active and below 7.0 were considered inactive and rests were moderately active. The dataset was divided randomly into training set and test set by considering the 75% of the total molecules in the training set and 35% in the test set.

Pharmacophore Hypotheses Generation

PHASE can identify the spatial arrangements of functional groups that are common and essential for the biological activity of the ligands used in the study [18]. Next step to develop pharmacophore model after preparing ligands is to create sites. The pharmacophore sites were created from a set of five pharmacophore features, including hydrogen

bond acceptor (A), hydrogen bond donor (D), hydrophobic group (H), and aromatic ring (R) by setting the pharmacophorematching tolerance to 1.2A°. Hypotheses were generated (see table 2) by variation of number of sites and the number of matching active compounds and common pharmacophore hypotheses were considered, which indicated at least five sites common to all molecules. Correlating the observed and the estimated activity for the training set performed the evaluation of generated common pharmacophore hypothesis. Finally, common pharmacophore hypothesis with significant statistical values were selected for molecular alignments. Survival score measures the quality of alignment and the best common pharmacophore hypothesis with highest survival score is selected. In the hypothesis scoring step default parameters for site, number of matches, vector, volume, selectivity and energy terms. Score hypotheses step is employed to align the actives to the hypotheses and calculate the score for the actives. Each pharmacophore and its associated ligand were treated temporarily as reference and assigned a score according to the alignment score, vector score and a volume score.

All the pharmacophore hypotheses were then used to build 3D QSAR models. The regression analysis was performed in which a series of models were constructed with an increasing number of PLS factors until over fitting starts to occur. Pharmacophore-based 3D-QSAR models were generated for the hypothesis using the 18 member training set with PLS factors of 2 and a grid spacing of 1.2A°.

Validation of Pharmacophore hypothesis

The external validation is considered to be a conclusive proof to determine the predictability of a model for which the data set has to be divided into training set and test set. The training set was used to generate pharmacophore model. Validation is an important aspect of pharmacophore design when the model is built for the purpose of predicting activities of molecules in external test set [19, 20]. In the present work, the developed pharmacophore model was externally validated by predicting the activity of test set molecules. The correlation between the experimental and predicted activities of the molecules of training and test sets are shown in tables 4a and 4b. The graphical representations are shown in figures 4a and 4b.

Molecular docking study

In the present study, we performed docking of the best fitted ligand in 3D-QSAR model i.e., compound 11 (Figure 2) into the active site of the mutated B-Raf^(V600E) kinase (PDB ID: 4FK3). The crystal structures of these proteins were downloaded from protein data bank. Protein preprocessing, optimization and minimization were carried out in the protein preparation wizard using OPLS-2005 force field and RMSD of 0.30A°. Grid was generated by using centroid of selected residue in the receptor grid generation panel by specifying the active site range as Leu525 - His540 residues. Finally impact minimised ligands were docked into the grid generated 4FK3 active site residues using the extra precision docking mode in GLIDE 5.7.

Table 2: Parameters of three featured pharmacophore hypotheses

gou	Hypothesis	SD	Survival score	R-squared	F	
1	ARRRR.3	0.1563	2.785	0.9825	420	
2	AARRR.2	0.1926	2.734	0.9734	274.1	
3	ADRRR.45	0.1477	2.696	0.9843	470.9	
4	AADRR.72	0.1651	2.61	0.9804	375.6	
5	AAADR.4	0.1694	2.466	0.9794	356.3	
6	ADDRR.43	0.1062	2.443	0.9919	918.8	
7	AARRR.58	0.221	2.365	0.9649	206.3	
8	AADDR.3	0.192	2.275	0.9735	275.8	
9	AAARR.39	0.1398	2.274	0.986	527.1	
10	AAARR.35	0.1398	2.274	0.986	527.1	
11	AAADR.2	0.1418	2.21	0.9856	512.1	
12	AAADR.1	0.1418	2.21	0.9856	512.1	
13	DRRRR.2	0.148	2.199	0.9843	469	

Table 3: PLS statistical parameters of the selected QSAR model

ID	PLS Factors	SD	R ²	F	P	Stability	RMSE	Q ²	Pearson-R
ARRRR.3	1	0.3767	0.8913	131.2	4.032e-009	0.7422	0.7699	0.3346	0.8841
	2	0.1563	0.9825	420	6.779e-014	0.5966	0.7419	0.3822	0.8978
AARRR.2	1	0.3737	0.893	133.6	3.544e-009	0.7063	0.7519	0.3653	0.8509
	2	0.1926	0.9734	274.1	1.55e-012	0.5134	0.7322	0.3983	0.7795
ADRRR.45	1	0.3723	0.8938	134.7	3.331e-009	0.664	0.6947	0.4583	0.829
	2	0.1477	0.9843	470.9	2.913e-014	0.5418	0.7599	0.3518	0.7981
AADRR.72	1	0.3622	0.8995	143.2	2.146e-009	0.6614	0.6527	0.5219	0.898
	2	0.1651	0.9804	375.6	1.543e-013	0.6055	0.6283	0.557	0.8756
AAADR.4	1	0.3437	0.9095	160.8	9.233e-010	0.7247	0.6365	0.5453	0.9334
	2	0.1694	0.9794	356.3	2.275e-013	0.6825	0.6274	0.5582	0.8995
ADDRR.43	1	0.3147	0.9241	194.8	2.237e-010	0.6778	0.5065	0.712	0.9468
	2	0.1062	0.9919	918.8	2.053e-016	0.598	0.5382	0.6749	0.908 1
AARRR.58	1	0.3459	0.9083	158.5	1.023e-009	0.7094	0.6166	0.5732	0.8592
	2	0.221	0.9649	206.3	1.226e-011	0.6879	0.5829	0.6187	0.8732
AADDR.3	1	0.3379	0.9125	166.9	7.008e-010	0.7082	0.6398	0.5405	0.8989
	2	0.192	0.9735	275.8	1.483e-012	0.6471	0.6348	0.5477	0.882
AAARR.39	1	0.3407	0.9111	163.9	8.004e-010	0.6417	0.5715	0.6333	0.9318
	2	0.1398	0.986	527.1	1.267e-014	0.5381	0.4817	0.7396	0.9583
AAARR.35	1	0.3407	0.9111	163.9	8.004e-010	0.6417	0.5715	0.6333	0.9318
	2	0.1398	0.986	527.1	1.267e-014	0.5381	0.4817	0.7396	0.9583
AAADR.2	1	0.3275	0.9178	178.7	4.236e-010	0.7275	0.6193	0.5695	0.9142
	2	0.1418	0.9856	512.1	1.567e-014	0.675	0.6073	0.5861	0.9449
AAADR.1	1	0.3275	0.9178	178.7	4.236e-010	0.7275	0.6193	0.5695	0.9142
	2	0.1418	0.9856	512.1	1.567e-014	0.675	0.6073	0.5861	0.9449
DRRRR.2	1	0.343	0.9099	161.5	8.921e-010	0.6903	0.6556	0.5176	0.9442
	2	0.148	0.9843	469	3.003e-014	0.5654	0.5586	0.6498	0.9535

SD: standard deviation of the regression, R: value of R^2 for the regression, F: variance ratio, large values of F indicate a more statistically significant regression, P: the significance level of variance ratio, smaller values indicate a greater degree of confidence, Stability: stability of the model predictions to changes in the training set composition, RMSE: Root-mean-square error, Q-squared: value of Q^2 for the predicted activities, Pearson-

RESULTS AND DISCUSSION

3D-QSAR Analysis

In this Ligand based pharmacophore model development, we developed a model, which screened important pharmacophoric features necessary for a group of napthol derivatives to function as inhibitors. Among the 18 compounds in training set, 5 were active and 13 were inactive and test set comprised of 6 compounds. The hypothesis (ADDRR.43) aligned with the best

fit ligand is shown in Figure 3. This hypothesis depicted a decent survival score (2.443), best regression coefficient (R^2 = 0.9919), highest variance (F = 918.8), and Standard deviation (SD = 0.1062) (Table 3). The squared predictive correlation coefficient (Q^2) for this model is 0.6749. Studies show that for a reliable model, the Q^2 should exceed 0.60 [21-22].

The distances (Figure 5) and angles between different sites of ADDRR.43 are given in Tables 5a and 5b. For each ligand, one

Figure 2: Structures of compound 11

(E)-N-(2-(dimethylamino)vinyl)-3-((5-hydroxynaphthalen-2-yl)amino)furo[2,3-c]pyridine-2-carboxamide

aligned conformer based on the lowest RMSE of feature atom coordinates from those of the corresponding reference feature was superimposed on ADDRR.43 and the fitness scores for all ligands were observed. The activity of a compound depends on fitness score, the greater the fitness score, greater the activity prediction of the compound. The fit function checks if the feature is mapped or not and also contains a distance term, which measures the distance that separates the features on the molecule from the centroid of the hypothesis feature. Table 4a shows the fitness score for all the molecules of training set. Beside this survival score analysis, another validation method to characterize the quality of *ADDRR.43* is represented by its capacity for correct activity prediction of training set molecules.

According to the results of this study, model ADDRR.43 can best fit for the prediction of B-Raf^(V600E) antagonistic activity. After analysis of the alignment between the active ligands and the generated hypothesis, a best hypothesis ADDRR.43 was selected for further research. The fitness between the most active ligand (compound 11) with hypothesis ADDRR.43 was 3.0 and the most inactive ligand (compound 33) was 0.46 as shown in Table 4a.

Hydrogen Bond Donor Field Predictions

The 3D-QSAR model shown in Figure 6a depicts hydrogen bond donor field prediction. Blue region near and around the OH at position D5 and N at D7 position indicates that the substitutions at these positions by groups having more hydrogen bond donor property are favorable for the B-Raf^(V600E) antagonistic activity. Red region around the H at D7 and N at A1 position indicates that substitutions at these positions by groups having hydrogen bond donor property are not favorable.

Hydrophobicity Field Prediction

The 3D-QSAR model shown in Figure 6b depicts the hydrophobicity field prediction. Blue regions indicate that the substitutions at these positions by groups having more hydrophobic characteristics favor B-Raf^(V600E) antagonistic activity. Red regions indicate that groups having more hydrophobic property do not favor B-Raf^(V600E) antagonistic activity.

Figure 3: Best pharmacophore model ADDRR.43 aligned with compound 11. Pharmacophore features are color coded: 1 hydrogen bond acceptors (A1; pink), 2 hydrogen bond donors (D5, D7; blue), and 2 aromatic rings (R11, R12; orange).

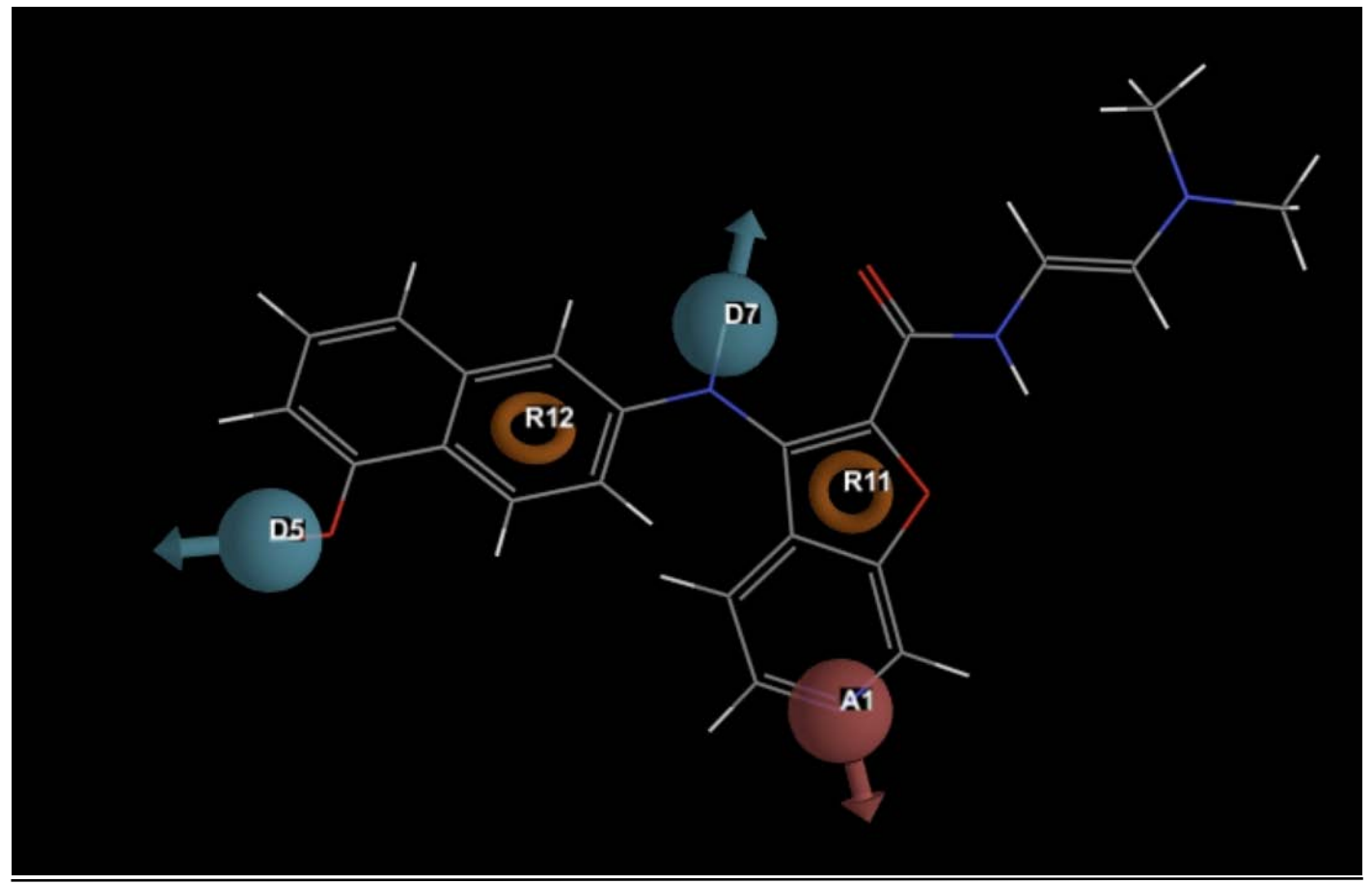
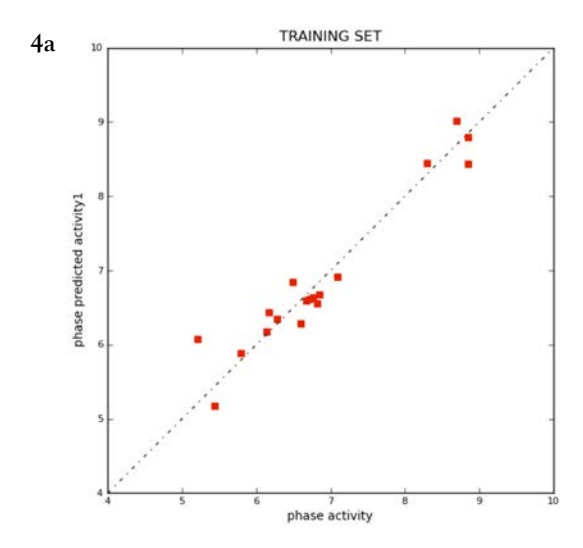
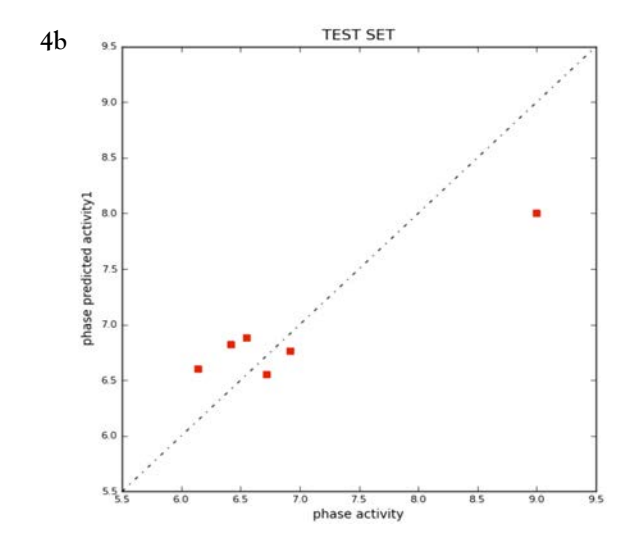


Figure 4a and 4b: Relation between experimental and predicted B-Raf^(V600E) antagonistic activity values of (a) training set and (b) test set molecules using model ADDRR.43





Docking Analysis

The XP G score of 8.81 kcal/mol was obtained in the docking study of compound 11 with 4FK3 protein [23]. The Binding model between compound 11 with active site residues is shown in Figure 7. Here, we found hydrogen bonding specifically between the oxygen moiety of OH group at D5 site with Asp594

(bond distance: 2.226 A°) and nitrogen(N) at A1 site with Cys532 (bond distance: 2.120 A°). Hence compound 11 (IUPAC name: (E)-N-(2-(dimethylamino)vinyl)-3-((5-hydroxynaphthalen-2-yl)amino)furo[2,3-c]pyridine-2-carboxamide), which is obtained by substituting (E)-N-(2-(dimethylamino) vinyl) acetamide at 'R' position of 6-(furo [2, 3-C] Pyridin-3-ylamino) naphthalene-1-ol

Table 4a: Experimental and predicted IC₅₀ values of training set molecules based on hypothesis ADDRR.43

Serial No.	Ligand Name	Experimental Activity (IC ₅₀)	Predicted Activity (IC ₅₀)	Pharm Set	Fitness
1	10	8.854	8.90	active	1.5
2	2	6.769	6.70	inactive	1.27
3	11	8.301	8.44	active	3
4	12	8.854	8.81	active	1.54
6	14	8.699	8.67	active	1.51
7	24	6.721	6.70	inactive	1.36
8	25	5.215	5.29	inactive	1.22
10	27	6.495	6.70	inactive	1.16
13	30	6.602	6.49	inactive	1.1
16	33	6.854	6.83	inactive	0.46
17	34	6.678	6.68	inactive	0.94
18	35	5.796	5.70	inactive	1.23
19	36	6.143	6.22	inactive	1.01
20	37	5.444	5.62	inactive	1.25
21	38	6.284	6.16	inactive	0.96
22	39	6.174	6.18	inactive	1.16
23	40	7.097	7.04	active	0.89
24	41	6.824	6.69	inactive	0.96

^{*}values highlighted in blue are those of the best fit and least fit ligands

Serial No.	Ligand Name	Experimental Activity	Predicted Activity	Pharm Set	Fitness	
1	13	9	7.95	active	1.22	
2	26	6.42	6.69	inactive	1.16	
3	28	6.921	6.79	inactive	1.32	
4	29	6.721	6.36	inactive	0.8	
5	31	6.553	6.86	inactive	1.11	
6	32	6.143	6.71	inactive	1.33	

Table 4b: Experimental and predicted IC₅₀ values of test set molecules based on hypothesis AADRR.43

performs the most potent activity which can be further concluded by invitro studies.

The protein B-Raf(V600E) is known to have an ATP binding pocket called "Raf selective pocket" formed by hydrophobic residues Thr529, Leu514, Phe595, Gly593, and Leu505 shown in Figure 7. Previous research revealed that this pocket is 11A° long with the side chain of residue Asp594 and other main chain atoms outlining the interior [24]. The binding model of compound 11 shows that it selectively binds to the ATP-binding site of B-Raf^(V600E), which confirms the importance of hydrophobic group in this inhibitor as shown in Figure 7. Studies have shown that the hydrophobic interactions between the inhibitor site and the receptor pocket are important for increasing the transactivation activity of Protein [25]. Studies also revealed that ATPcompetitive, small molecule inhibitors of B-Raf^(V600E) kinase have the potential for anti-neoplastic activity. One such example is the drug Vemurafenib, which also selectively binds to the ATPbinding site of B-Raf^(V600E) kinase expressed in tumor cells and helps in reduction of tumor cell proliferation.

The residue Asp594 plays a very important role in switching active and inactive conformations of B-Raf^(V600E) protein. Asp594, which is present in the activation segment approaches α -C helix and places residue Glu600 in the proximity of the aliphatic region of Lys507 of the α -C helix facilitating salt bridge interactions between them. These interactions make the B-Raf^(V600E) active. Docking studies also reveal that compound 11

Table 5a: Distances between different sites of

Table 5b: Angles between different sites of model ADDRR.43

model AI	DDRR.43	,			o. migic	.s Detwee	.ii dilici	ciit sites (or mode.	MDDK	.10.75		
S.No.	Site-1	Site-2	Distance (A°)	S.No	Site1	Site2	Site3	Angle	S.No	Site1	Site2	Site3	Angle
				1	D5	A1	D7	55.9	16	D5	D7	R11	101
1	A1	D5	9.525	2	D5	A1	R11	72.4	17	D5	D7	R12	5.7
2	A1	D7	6.194	3	D5	A1	R12	25.5	18	R11	D7	R12	98.2
				4	D7	A1	R11	20	19	A1	R11	D5	86.5
3	A1	R11	3.449	5	D7	A1	R12	30.6	20	A 1	R11	D7	138.2
4	A1	R12	6.514	6	R11	A1	R12	48.4	21	A1	R11	R12	100.2
				7	A1	D5	D7	40.3	22	D5	R11	D7	59
5	D5	D7	7.937	8	A1	D5	R11	21.2	23	D5	R11	R12	17.1
6	D5	R11	9.095	9	A1	D5	R12	37.6	24	D7	R11	R12	42.3
7	D5	R12	4.602	10	D7	D5	R11	20.1	25	A1	R12	D5	116.9
1	כט			11	D7	D5	R12	4.1	26	A1	R12	D7	69.4
8	D7	R11	3.181	12	R11	D5	R12	18.4	27	A1	R12	R11	31.4
9	D7	R12	3.363	13	A1	D7	D5	83.8	28	D5	R12	D7	170.2
				14	A1	D7	R11	21.8	29	D5	R12	R11	144.5
10	R11	R12	4.948	15	A1	D7	R12	80	30	D7	R12	R11	39.5

binds proximal to the ATP binding cleft of B-Raf^(V600E) located between the N-lobe and C-lobe of the kinase domain as shown in Figure 8. The rest of the inhibitor molecule largely occupies the hydrophobic space formed proximal to the hinge region of the N-lobe and C-lobe, orthogonal to the P-loop extension.

CONCLUSION

Studies have shown that B-Raf^(V600E) mutation exhibited clear evidence of being an active target for human melanoma cancer. B-Raf^(V600E) inhibitors are potential therapeutic drugs that can inhibit the expression of mutated B-Raf protein thereby playing an important role in treatment of cancer. This study shows the generation of a pharmacophore model ADDRR.43 for Naphthol derivatives acting as B-Raf^(V600E) antagonists. Pharmacophore modelling correlates activities with the spatial arrangement of various chemical features. The ADDRR.43 pharmacophore model is able to accurately predict B-Raf^(V600E) antagonistic activity, and the validation results also provide additional confidence in the proposed pharmacophore model. The obtained results suggested that the proposed 3D-QSAR model can be useful to rationally design new Naphthol derivatives molecules as B-Raf^(V600E) antagonists.

Moreover, docking evidences reveals extensive and specific interactions between compound 11 and the ATP binding pocket of the B-RAF kinase domain, establishing compound 11 as an ATP competitive inhibitor and confirming its potent inhibitory properties against B-Raf^(V600E). Since Asp594 adopts distinct

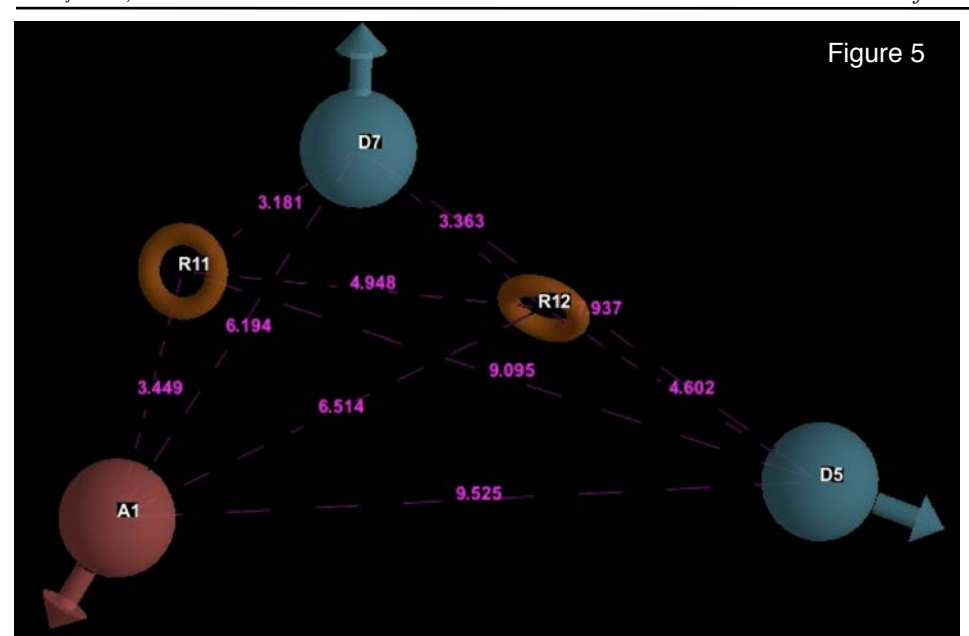


Figure 5: PHASE-generated pharmacophore model ADDRR.43 illustrating hydrogen bond acceptor (A1; pink), hydrogen bond donor (D5, D7; blue), and aromatic ring (R11, R12; orange) features showing distances (in A°)

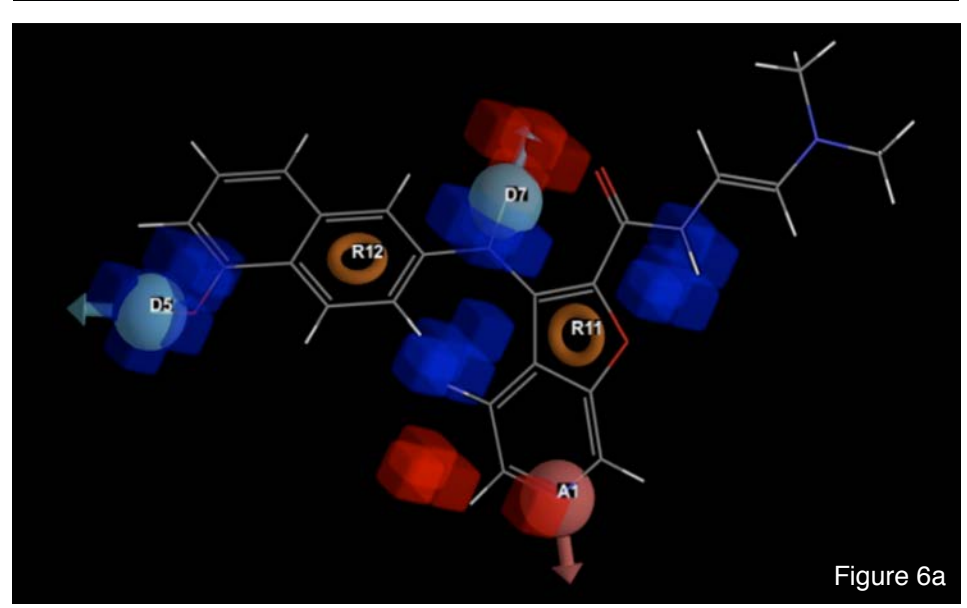


Figure 6a and 6b: 3 D-Q SAR visualization model based on compound 11 of training set illustrating.

6a. Hydrogen bond donor feature and 6b. Electron withdrawing characteristics and hydrophobicity features.

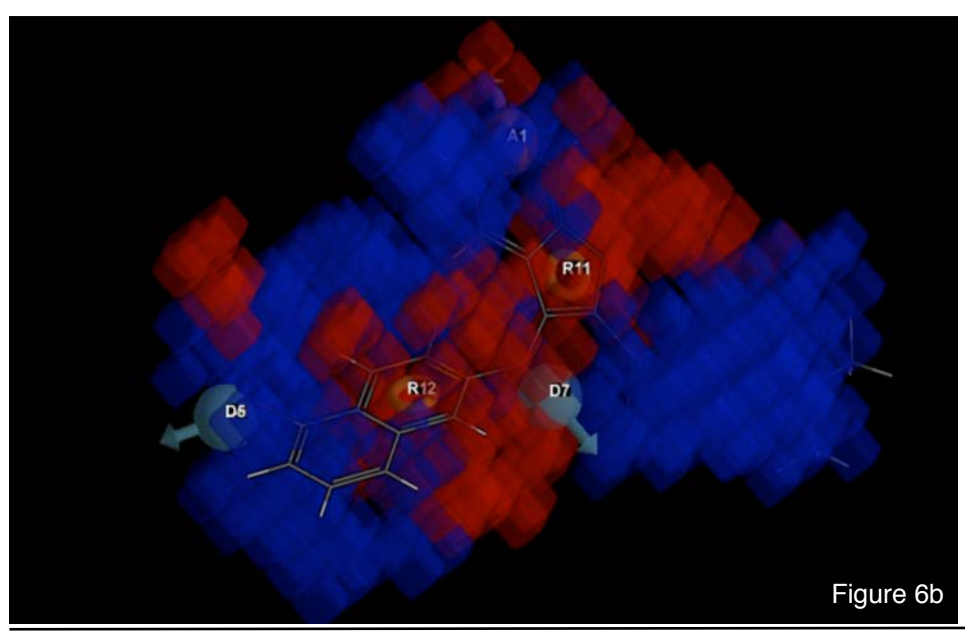


Figure 7: Binding interaction of compound 11 with the B-Raf^(V600E) in the RAF selective pocket. Hydrogen bond interactions with active sites CYS 532 and ASP 594 are represented in pink dotted lines.

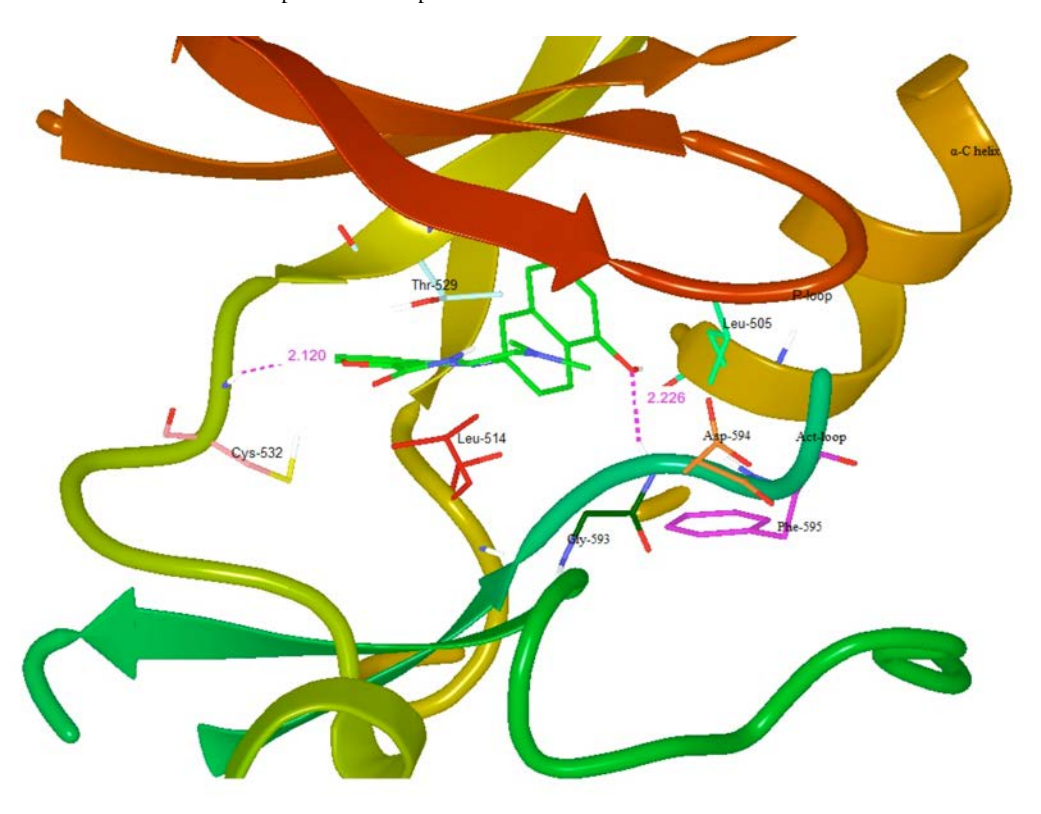
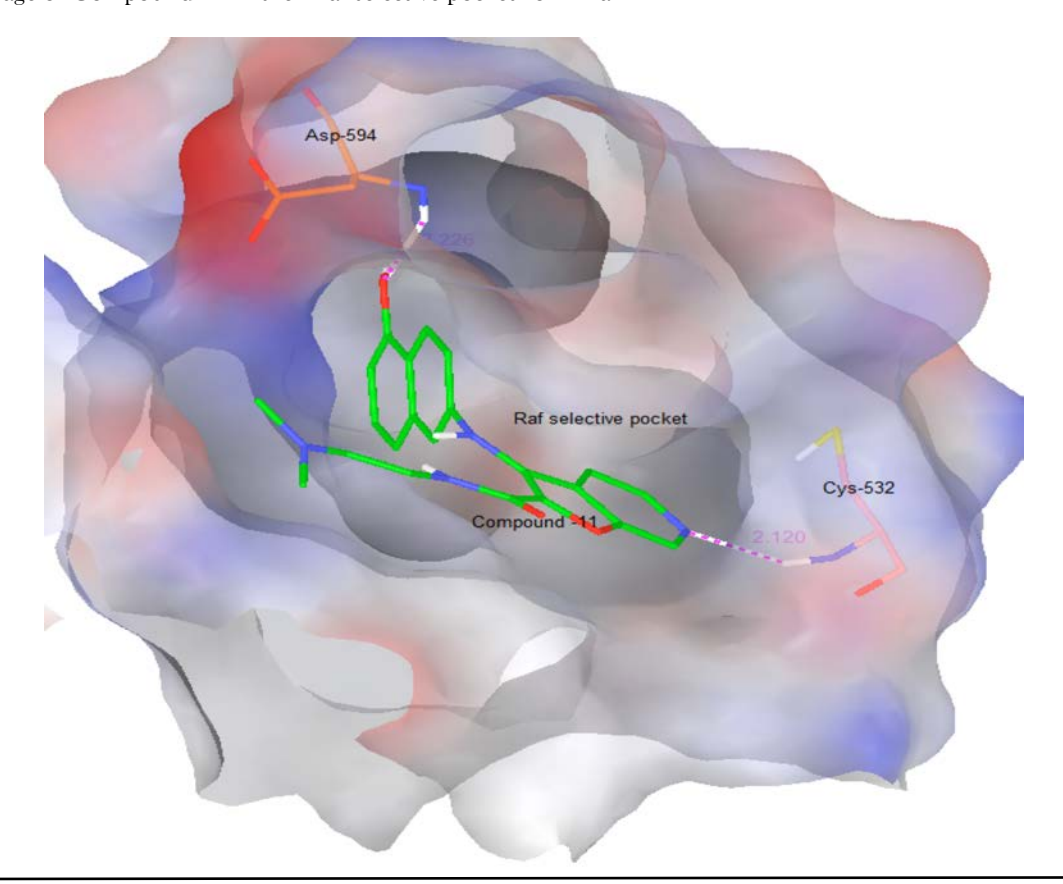


Figure 8: Docking image of Compound 11 in the "Raf selective pocket" of B-Raf^(V600E)



conformations in the active B-Raf^(V600E) conformation compared to the inactive B-Raf^(V600E) conformation, Designing a linker supporting the protrusion into the Raf-specific pocket while it still interacts with the active conformation of Asp594 will most likely improve the selectivity of the next generation of inhibitors against the B-Raf^(V600E) oncogenic mutant kinase over the wild-type enzyme.

Acknowledgement

We thank Raghu Rangaswamy, Senior Director and Vinod Devaraji IT consultant from Schrödinger for providing academic evaluations software and continuous support to undertake this research work.

REFERENCES

- 1. Dienstmann R, Tabernero J: B-RAF as a target for cancer therapy. Anticancer Agents in Medicinal Chemistry 2011, 11:285-295.
- Matallanas D, Birtwistle M, Romano D, Zebisch A, Rauch J, Von AK, Kolch W: Raf family kinases: old dogs have learned new tricks. Genes Cancer 2011, 2: 232-260.
- 3. Pasha FA, Muddassar M, Neaz MM, Cho SJ: Pharmacophore and docking-based combined in-silico study of KDR inhibitors. *Journal of Molecular Graphics & Modelling* 2009, 28:54-61.
- Guner OF: Pharmacophore Perception, Development and Use in Drug Design. International University Line, San Diego, Calif, USA, 2000.
- 5. Nielsen TE, S.L. Schreiber, Towards the Optimal Screening Collection: A Synthesis Strategy. Angewandte Chemie Inernaional Ed. in English 2008, 47: 48-56.
- Langer T, Eder M, Hoffmann RD, Chiba P, Ecker GF: Lead identification for modulators of multidrug resistance based on insilico screening with a pharmacophoric feature model. Archiv dar Pharmazie 2004, 337:317-327.
- Ke YY, Shiao HY, Hsu YC, Chu CY, Wang WC, Lee YC, Lin WH, Chen CH, Hsu JT, Chang CW, Lin CW, Yeh TK, Chao YS, Coumar MS, Hsieh HP: 3D-QSAR-Assisted Drug Design: Identification of a Potent Quinazoline-Based Aurora Kinase Inhibitor. ChemMedChem 2013, 8:136-148.
- Debnath AK: Application of 3D-QSAR techniques in anti-HIV-1 drug design-an overview. Current Pharmaceutical Design 2005, 11:3091-3110.
- Zhang N, Jiang Y, Zou J, Zhang B, Jin H, Wang Y, Yu Q: 3D QSAR for GSK-3beta inhibition by indirubin analogues. European Journal of Medicinal Chemistry 2006, 41:373-378.
- 10. Yong A, Shao TW, Chu T, Sun PH, Song FJ: 3D-QSAR and docking studies on pyridopyrazinones as BRAF inhibitors. Medicinal Chemistry Research 2011, 20:1298-1317.
- 11. Duchowicz PR, Castro EA: QSAR studies for the pharmacological inhibition of glycogen synthase kinase-3. Medicinal Chemistry 2007, 3:393-417.

- 12. Liu GY, Ju XL, Cheng J, Liu ZQ: 3D-QSAR studies of insecticidal anthranilic diamides as ryanodine receptor activators using CoMFA, CoMSIA and DISCOtech. Chemosphere 2010, 78:300-306.
- 13. Peng Y, Keenan SM, Zhang Q, Kholodovych V, Welsh WJ: 3D-QSAR comparative molecular field analysis on opioid receptor antagonists: pooling data from different studies. Journal of Medicinal Chemistry 2005, 48:1620-1629.
- 14. Qin J, Xie P, Ventocilla C, Zhou G, Vultur A, Chen Q, Liu Q, Herlyn M, Winkler J, Marmorstein R: **Identification** of a novel family of BRAF(V600E) inhibitors. *Journal of Medicinal Chemistry* 2012, 55:5220-5230.
- 15. Ren L, Wenglowsky S, Miknis G, Rast B, Buckmelter AJ, Ely RJ, Schlachter S, Laird ER, Randolph N, Callejo M, Martinson M, Galbraith S, Brandhuber BJ, Vigers G, Morales T, Voegtli WC, Lyssikatos J: Non-oxime inhibitors of B-Raf(V600E) kinase. Bioorganic & Medicinal Chemistry Letters 2011, 21:1243-1247.
- 16. Dixon SL, Smondyrev AM, Knoll EH, Rao SN, Shaw DE, Friesner RA: PHASE: a new engine for pharmacophore perception, 3D QSAR model development, and 3D database screening: 1. Methodology and preliminary results. Journal of Computer-Aided Molecular Design 2006, 20:647-671.
- 17. Yang YS, Li QS, Sun S, Zhang YB, Wang XL, Zhang F, Tang JF, Zhu HL: Design, modification and 3D QSAR studies of novel 2,3-dihydrobenzo[b][1,4]dioxincontaining 4,5-dihydro-1H-pyrazole derivatives as inhibitors of B-Raf kinase. Bioorganic & Medicinal Chemistry 2012, 20:6048-6058.
- Evans DA, Doman TN, Thorner DA, Bodkin MJ: 3D QSAR methods: phase and catalyst compared, *Journal of Chemical Information and Modeling* 2007, 47:1248–1257.
- 19. Schüürmann G, Ebert RU, Chen J, Wang B, Kühne R: External Validation and Prediction Employing the Predictive Squared Correlation Coefficient Test Set Activity Mean vs Training Set Activity Mean. Journal of Chemical Information and Modeling 2008, 48:2140–2145.
- Boyd DB: Successes of Computer-Assisted Molecular Design. In Reviews in Computational Chemistry, K.B. Lipkowitz and D. B. Boyd, Eds., VCH Publishers, New York, 1990, Vol. 1, pp. 355-371.
- Dureja H, Kumar V, Gupta S, Madan AK: Topochemical models for the prediction of lipophilicity of 1, 3disubstituted propan-2-one analogs. Journal of Theoretical and Computational Chemistry 2007, 6:435– 448.
- Wold S: Validation of QSAR's. Quantitative Structure-Activity Relationships. 1991, 10:191–193.
- 23. Meraj K, Mahto MK, Christina NB, Desai N, Shahbazi S, Bhaskar M: Molecular modeling, docking and ADMET studies towards development of novel Disopyramide analogs for potential inhibition of human voltage gated sodium channel proteins. Bioinformation 2012, 8:1139-1146.
- 24. Xie P, Streu C, Qin J, Bregman H, Pagano N, Meggers E,

Marmorstein R: The Crystal Structure of BRAF in Complex with an Organoruthenium Inhibitor reveals a Mechanism for Inhibition of an Active Form of BRAF Kinase. *Biochemistry* 2009, 48:5187–5198.

25. Guasch L, Sala E, Valls C, Mulero M, Pujadas G, Garcia-Vallve S, Development of docking-based 3D-QSAR models for PPARgamma full agonists. *Journal of Molecular Graphics & Modelling* 2012, 36:1–9.

<u>Note:</u> Vedic Research International, Vedic Research Inc is not responsible for any data in the present article including, but not limited to, writeup, figures, tables. If you have any questions, directly contact authors.

Authors Column



Manoj Kumar Mahto persueing his Ph.D. degree in Bioinformatics from the Nagarjuna University, Dept. of Biotechnology, Guntur (A.P). He has completed his M.Sc. in Bioinformatics from Sikkim Manipal University. He has also completed his P.G. Diploma in Bioinformatics from University of Mysore. He is having an Experience of 8 years in the field of Bio, Chem, Immuno and Medical informatics. He has worked on various Projects of Homology Modeling, Novel lead designing, Docking studies, 3D QSAR studies, Immunoinformatics, PERL, BIOPERL, Micro Array Gene Expression Analysis and Drug Designing. He has been invited as a Guest faculty in various Universities of India. He is having very good research aptitude with quality publications.